# Interactions of cholesterol esters with phospholipids: cholesteryl myristate and dimyristoyl lecithin

**Martin J. Janiak,[1] Donald M. Small, and G. Graham Shipley[2]**

Biophysics Division, Departments of Medicine and Biochemistry, Boston University School of Medicine, Boston, MA 02118

**Abstract** The ternary phase diagram of cholesteryl myristate–dimyristoyl lecithin–water has been determined by polarizing light microscopy, scanning calorimetry, and x-ray diffraction. Hydrated dimyristoyl lecithin forms a lamellar liquid–crystalline phase ($L_\alpha$) at temperatures >23°C into which limited amounts of cholesteryl myristate (<5 wt.%) can be incorporated. The amount of cholesterol ester incorporated is dependent upon the degree of hydration of the $L_\alpha$ phase. Below 23°C dimyristoyl lecithin forms ordered hydrocarbon chain structures ($L_{\beta'}$ and $P_{\beta'}$) which do not incorporate cholesterol ester. Comparison with other phospholipid–cholesterol ester–water phase diagrams suggests the following general principles: *i*) the incorporation of cholesterol ester occurs only into liquid crystalline phospholipid bilayers, *ii*) the extent of incorporation is temperature-dependent, with increasing amounts of cholesterol ester being incorporated at higher temperatures, and *iii*) unsaturated cholesterol esters induce increased disordering of the phospholipid bilayers.—**Janiak, M. J., D. M. Small, and G. G. Shipley.** Interactions of cholesterol esters with phospholipids: cholesteryl myristate and dimyristoyl lecithin. *J. Lipid Res.* 1979. **20:** 183–199.

**Supplementary key words** atherosclerosis · cell membranes · differential scanning calorimetry · liquid crystalline mesophases · order–disorder phenomena · phase equilibria · polarizing light microscopy · x-ray diffraction

The structural and metabolic interrelationships of systems involved in lipid transport and storage processes are complex. For example, different amounts of phospholipids, cholesterol, cholesterol esters, and triglycerides, in association with protein, are transported in specific plasma lipoproteins through the bloodstream (1) and high concentrations of these lipids are found in tissues such as the adrenal cortex (2) and ovaries (3). In normal arterial tissue there is an age-related increase in lipid content (4). Of particular importance is the abnormal, localized accumulation or deposition in arterial tissue of lipids, rich in cholesterol esters and phospholipids, which results in "fatty streak" intimal lesions. These early lesions may eventually develop into more severe lesions or plaques associated with arterial blockage and atherosclerosis (5–7). Recently, we characterized the interrelationships of the major lipids accumulating in atherosclerotic lesions (8) and have shown that the development of these lesions may be explained in physicochemical terms, at least for their lipid components (8, 9).

A critical part of these studies was the demonstration that unsaturated cholesterol esters have limited solubility in hydrated phospholipid bilayers (10). We have now examined the interaction between cholesteryl myristate and dimyristoyl lecithin, a system in which the fatty acid component of the two lipids is constant. This, together with our earlier studies, enables us to discuss a general theory for the interaction of these two biologically important lipid classes.

## MATERIALS AND METHODS

### Materials

Cholesteryl myristate (CM) was obtained from Nu Chek Prep (Elysian, MN) and was determined to be greater than 99% pure by chromatographic methods. Thin-layer chromatography (TLC) showed only a single spot corresponding to cholesterol ester and gas–liquid chromatography (GLC) revealed only minor contamination (<1%) by other fatty acids. Dimyristoyl lecithin (DML) was synthesized from glycerophosphorylcholine prepared from a choline phosphoglyceride isolated from egg yolk (11) and myristic acid (Nu Chek Prep) by the method of Cubero Robles and Van Den Berg (12). DML was isolated by silicic acid chromatography and determined to be only phosphatidylcholine by TLC, with a fatty acyl

Abbreviations: CM, cholesteryl myristate; DML, dimyristoyl lecithin; TLC, thin-layer chromatography; GLC, gas-liquid chromatography; DSC, differential scanning calorimetry; CE, cholesterol ester; PL, phospholipid.

[1] Present address: Rigaku/U.S.A., Inc., Danvers, MA 01923.

[2] To whom correspondence should be addressed.

composition consisting of 99.9% myristate as judged by GLC.

### Preparation of mixtures

Cholesteryl myristate and dimyristoyl lecithin were weighed into a flask and dissolved in chloroform–methanol 2:1 (v/v) to give a bulk solution containing a specific ratio of CM:DML ($X$% CM:100 − $X$% DML). Aliquots from each bulk solution were transferred to glass tubes with a central constriction. The solvent was evaporated in vacuo and a predetermined amount of water was added to each dry mixture. Thus, each specific weight ratio of CM:DML was prepared as a series of increasing water concentrations, the composition of each mixture being referred to as $a$% water: (100 − $a$%) total lipid, where the ratio of CM:DML of total lipid is given by ($X$% CM:100 − $X$% DML).

Rapid equilibration of this mixed lipid system occurs when both components exist in a disordered liquid–crystalline or liquid state. However, equilibration of mixtures of cholesteryl myristate and dimyristoyl lecithin is complicated due to the high temperature of the liquid crystal to isotropic liquid transition of cholesterol ester (85.5°C). In the absence of cholesterol esters, even at moderate temperatures (~50°C), hydrolysis of DML occurs after about 6 hr with detectable traces of lysolecithin being formed (0.2–0.5%). For this reason a modified equilibration procedure was used. After sealing the glass tube, the sample was centrifuged (1000 $g$) through the central constriction for 3 min at 90°C during which time the CM melted and the sample appeared homogeneous. The sample was then immediately transferred to a second centrifuge operating at 50°C and equilibrated by centrifugation (1000 $g$) through the constriction for 4–5 hr at this temperature. All samples studied contained 0.5–1.0% lysolecithin. However, of several equilibration methods investigated, this procedure resulted in minimum sample degradation and ensured sample homogeneity and reproducible observations by polarizing light microscopy, scanning calorimetry, and x-ray diffraction. Further, the presence of this small amount of lysolecithin did not affect the phase behavior of hydrated DML as determined by parallel control studies.

Immediately on opening the constricted tube, a well-mixed sample of the mixture was weighed, dried in vacuo, and reweighed to determine the water content gravimetrically. Each mixture was examined by polarizing light microscopy, differential scanning calorimetry, and x-ray diffraction.

### Polarizing light microscopy

Each sample was placed between a slide and coverslip and immediately examined by direct light and between crossed nicols in a Zeiss standard NL microscope. A gross estimate of the viscosity of the sample was obtained by pressing on the coverslip and deforming the sample. The sample was initially examined at a temperature 2–5°C above the chain-melting transition of hydrated DML and the textural appearance and number of phases were recorded. The sample was then heated to 90°C (heating rate 1–2°C/min) to identify any changes in appearance of the sample, noting in particular the presence of any CM thermal transitions. The sample was then cooled to the starting temperature and repeatedly heated and cooled, noting the reproducibility of these changes. Samples that exhibited only one phase were cooled to −10°C, held at this temperature for 1 hr, and then re-examined in the same fashion, noting any textural difference. A second sample was examined between 5 and 90°C in a similar fashion. To a third sample, water was added at 5°C and heated to determine the temperature at which growth of myelin figures occurred.

### Differential scanning calorimetry (DSC)

Samples taken for calorimetry (5–10 mg) were hermetically sealed in aluminum pans and placed in a Perkin–Elmer (DSC-2) differential scanning calorimeter. Samples were studied at variable heating/cooling rates from 1.25 to 10°C/min. Each sample was heated from the equilibration temperature to 90°C, cooled to 0°C, and then repeatedly heated and cooled between 0°C and 90°C.

### X-ray diffraction

The x-ray source was an Elliott GX-6 rotating anode generator using nickel-filtered Cu-$K\alpha$ radiation, a 200-$\mu$m spot, and operating at 40 Kv, 40 mA. The x-ray beam was optically focused using modified double mirror (13) and toroidal (14) cameras (Baird and Tatlock, London). Unoriented specimens were contained in a sample holder adapted to either an electrical (range, ambient to 300°C; accuracy ± 2°C) or a circulating solvent (range −15 to 80°C, accuracy ± 0.1°C) variable temperature apparatus capable of operating with either camera. Specimens were contained either between two 50 $\mu$m Mylar windows (specimen thickness 2 mm) or in thin-walled capillary tubes (internal diameter 0.7 mm). The diffraction patterns were recorded using flat film cassettes with Ilford Industrial G photographic film.

## RESULTS

### Microscopic examination

*Cholesteryl myristate.* At 25°C, cholesteryl myristate forms a rigid birefringent texture containing spheru-

lites (**Fig. 1*a***). The sample remains unchanged in appearance until 70°C when homeotropic droplets form out of the birefringent continuum. On depressing the coverslip at 72°C, the sample flows and transforms to the smectic mesophase textures (Fig. 1*b*). At 79.5°C, the sample transforms to the fine birefringent textures of the cholesteric phase (Fig. 1*c*). At 85.0°C, there is a rapid loss of birefringence and the sample is completely isotropic by 86.0°C. If the sample is cooled from 90°C, these same liquid crystalline transitions and textures are observed with slight supercooling (~1°C). On further cooling of the sample, spherulite growth is observed at ~50°C. This temperature lies at the upper limit of the temperature range where nucleation is homogeneous (15). The textures observed here are similar to those reported by Barrall, Porter, and Johnson (16). The melting behavior of cholesteryl myristate was not influenced by the presence of water and the two components were immiscible in all proportions.

*Dimyristoyl lecithin–water*. We have established those structural changes associated with the thermal transitions of hydrated DML (17). Hydrated DML undergoes two thermal transitions, a broad low enthalpy "pre-transition" prior to the sharp first order "chain-melting" transition. Below the pretransition, a one-dimensional lamellar ($L_{\beta'}$) phase is observed with the hydrocarbon chains extended and tilted with respect to the normal to the plane of the lipid bilayer. The pretransition is associated with a structural transformation to a two-dimensional $P_{\beta'}$ phase consisting of lipid lamellae distorted by a periodic ripple with the hydrocarbon chains remaining tilted. At the chain-melting transition, the hydrocarbon chains assume a liquid-like conformation and the one-dimensional lamellar $L_\alpha$ phase is formed.

All mixtures of hydrated DML exhibit the same textural features at water contents >10%. At 5°C, DML appears as a waxy, highly birefringent "viscous neat" texture (18) as shown in Fig. 1*d*. On heating the sample, no change in appearance or birefringence occurs at the pretransition temperature (11°C). At the chain-melting transition (23°C), a marked decrease in the viscosity of the sample occurs, accompanied by a loss of birefringence and the appearance of homeotropic areas and focal conics of positive sign of birefringence, i.e., the "neat" textured phase. On continued heating, the neat texture assumes a well-defined network of "oily streaks" (ref. 18, see Fig. 1*e*). On heating to 90°C, the sample becomes more homeotropic with a further loss in birefringence.

In mixtures containing between 12 and 25% water, a significant decrease in the viscosity occurs at temperatures decreasing with increasing water content, from 35°C at 15% water to a limiting value of 25°C at 25% water. If water is added to the sample at 5°C, no water penetration or myelin figure growth occurs. If the sample is then heated, water penetrates at the sample edge at ~2°C below the softening temperature (25°C) and myelin figure growth occurs within 2°C of the softening temperature (see Fig. 1*f*). In mixtures containing >40% water, no penetration or growth of myelin figures was observed on addition of water, indicating that water was already present as a separate phase. Thus, the neat textured phase is associated with the structure $L_\alpha$ and viscous neat with $P_{\beta'}$ or $L_{\beta'}$.

*(2.79% CM:97.21% DML) 20% water*. At 35°C, the sample appears as a single phase (**Fig. 2*a***) and exhibits a birefringent neat texture (Fig. 2*b*). As the sample is heated to 90°C, a progressive loss in birefringence occurs. If the sample is cooled to −10°C and maintained at this temperature for 1 hr and then examined at 5°C, the sample exhibits a viscous-neat texture as observed for DML, but a second phase of small, highly birefringent angular grains is now present. On heating the sample from 5°C, a marked decrease in the viscosity occurs at 30°C and the sample assumes a neat texture. At 70–72°C, the birefringent angular grains melt to form droplets and are thus associated with cholesteryl myristate. No other changes were observed on heating to 90°C. If the sample is cooled from 90°C to between 40 and 50°C, and maintained at this temperature for several hours, the droplets slowly disappear and the sample eventually appears as one phase. If water is added to a sample at 5°C and then heated, water penetration occurs at 30°C and myelin figure growth at 32°C.

*(2.79% CM:97.21% DML) 50% water*. At 30°C, the sample contains three phases, a birefringent neat textured phase, cholesteryl myristate crystals, and water. As the sample is heated to 90°C, a progressive loss in birefringence occurs and large homeotropic areas are present. Between 70 and 72°C, the birefringent crystals melt to form homeotropic droplets which become birefringent between 78 and 80°C and exhibit a negative sign of birefringence. At 85°C, the droplets lose birefringence and become isotropic. At 87°C, the sample assumes a weakly birefringent neat texture (Fig. 2*c*). On cooling, birefringent droplets reappear abruptly at 84°C (Fig. 2*d*). This birefringence is lost at 78°C (Fig. 2*e*). Crystals of CM do not form spontaneously from the homeotropic droplets, but after about 1 hr at 25°C crystals are present. The transitions observed are reproduced on subsequent heating and cooling of the sample. If the sample is held at ~65°C on cooling from 90°C, the droplets appear to decrease in size after several hours but two phases remain. At 5°C, a birefringent viscous-neat textured

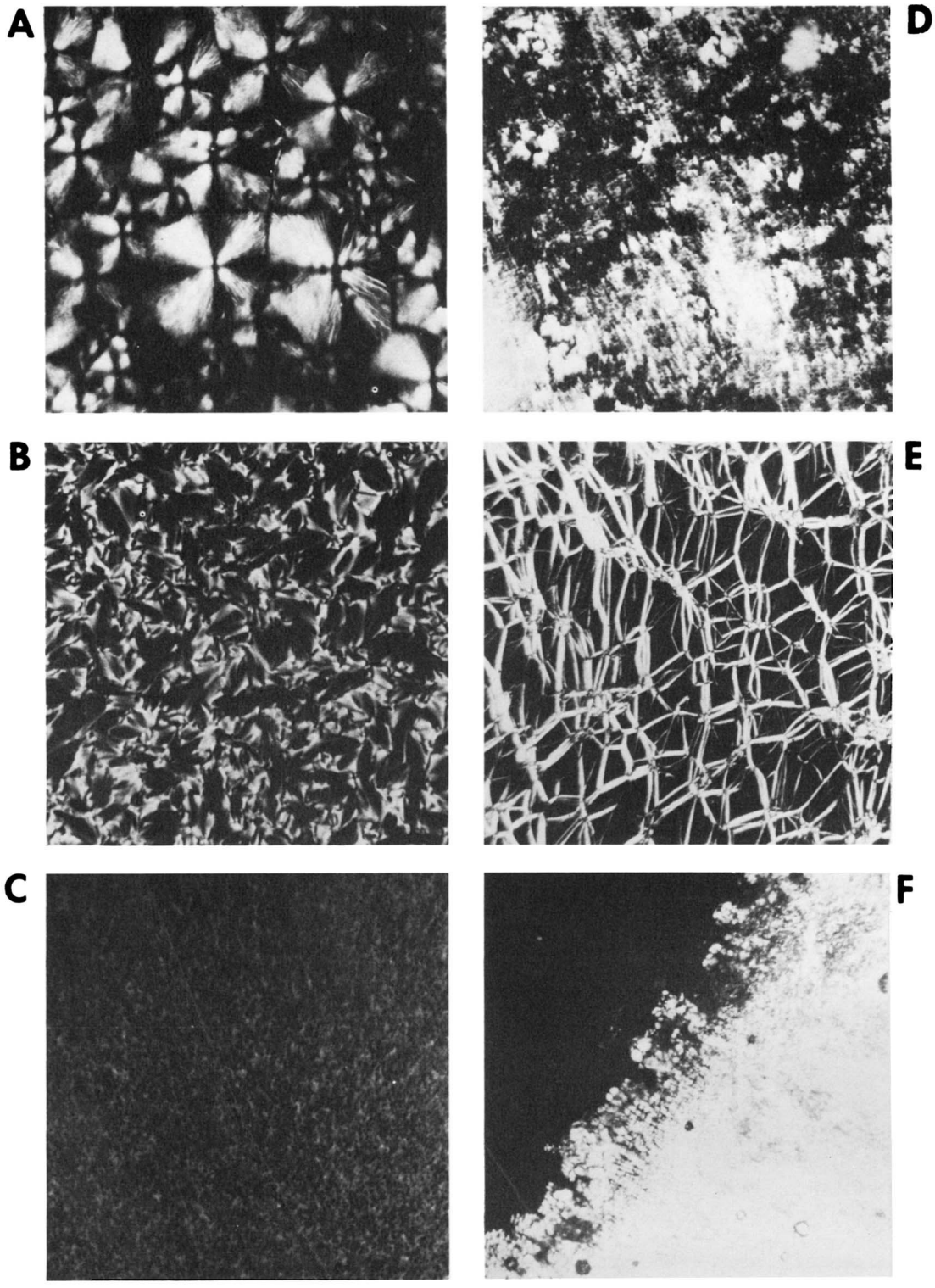


**Fig. 1.** Microscopically observed textures of CM (*a,b,c*) and DML containing 25% water (*d,e,f*); crossed polarizers, magnification 112×. For CM, (*a*) crystalline phase at 25°C, (*b*) smectic phase at 74°C, (*c*) cholesteric phase at 82°C. For DML, (*d*) "viscous neat" texture at 5°C, (*e*) "neat" texture at 60°C. In (*f*), addition of water produced the growth of myelin figures into the water phase at 28°C; sample photographed at 32°C. CM was recrystallized in situ. The heating rate was 1–2°C/min.

phase is present together with crystals of CM. On heating the sample, a marked decrease in the viscosity is observed at 25°C and the sample transforms to a neat textured phase. No myelin figure growth is observed at any temperature on addition of water since, at 50% water, the mixtures are always fully hydrated.

In general, mixtures of CM–DML–water exhibited the phase behavior of the separate components, i.e.,

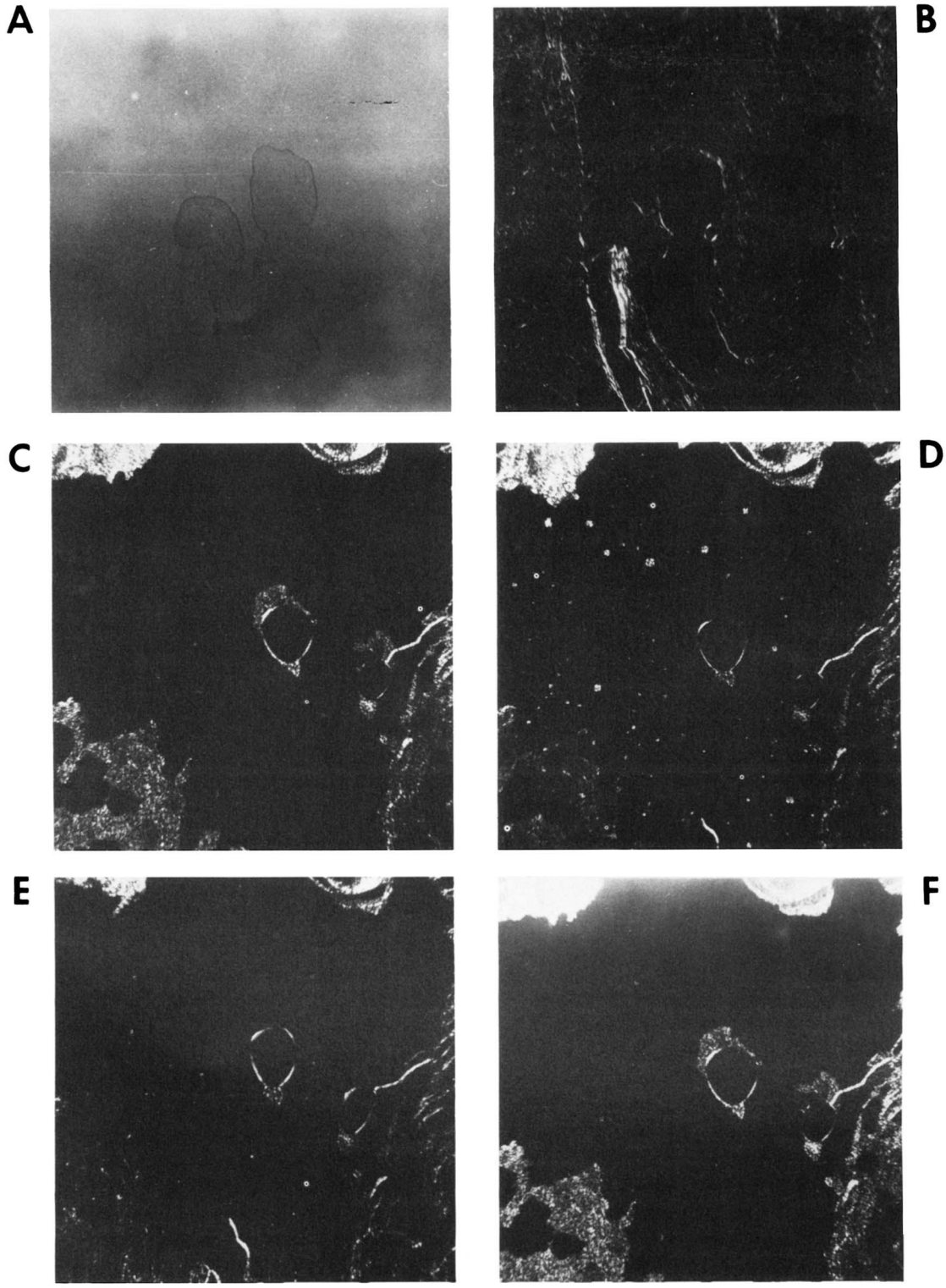


**Fig. 2.** Microscopically observed textures for mixtures of 2.79% CM:97.21% DML containing 20% water at 40°C (*a,b*) and 50% water at 87°C (*c*), 82°C (*d*), 78°C (*e*), and 76°C (*f*). (*a*) Direct light; (*b–f*) crossed polarizers; magnification 112×.

hydrated dimyristoyl lecithin and cholesteryl myristate. The transition from viscous-neat to neat texture for mixtures containing CM was observed within a degree of that found for DML at comparable water contents. Growth of myelin figures occurred at comparable temperatures providing water was not present as an excess phase. When a cholesterol ester phase was present, transitions from crystal to smectic and, except at very low ester contents, smectic to cholesteric and cholesteric to isotropic were observed. The liquid–

crystalline transitions temperatures (smectic to cholesteric and cholesteric to isotropic) were lowered by ~1°C in mixtures containing CM in comparison to CM alone. In addition, the domain size of the excess cholesterol ester phase appeared to diminish at higher temperature. The crystallization of ester from the liquid–crystalline phase was similarly dependent on domain size, crystallization of ester occurring more rapidly at higher ester content.

At 37°C, a number of changes were observed as the water content was increased in mixtures containing 2.79% CM:97.21% DML (**Fig. 3**). At low water contents (<16.4%), two phases were observed, a neat textured phase together with crystals of CM. Upon further increasing the water content (19.7% water), crystals of CM were no longer present. At higher water content (31.2%), two phases were again observed. All mixtures containing greater than 39.7% water contained three phases, the third phase being excess water. Similar behavior was observed in mixtures containing 1.71% CM:98.29% DML (Fig. 3).

In mixtures containing 5.5% CM:94.5% DML, no mixture produced only a single phase. Similarly, all mixtures containing greater than 5.5% CM:94.5% DML (10.7:89.3, 16.0:84.0, and 30.9% CM:69.1% DML) contained either two phases, neat and CM crystals, or three phases, the additional phase being water. At 10°C and 20°C, no mixtures showed only one phase. All mixtures contained either two phases, viscous-neat and CM crystals, or three phases, the additional phase being water.

## Differential scanning calorimetry

Typical DSC thermograms obtained for mixtures of CM:DML containing 30% water are shown in **Fig. 4***b*, *c*, and *d*. Mixtures containing 1.7% CM:98.3% DML (Fig. 4*b*) exhibit the same thermal behavior as hydrated DML alone (Fig. 4*a*). No thermal transitions arising from cholesteryl myristate could be detected (Fig. 4*e*). It is important to note that, at maximum sensitivity of the instrument where the crystal to

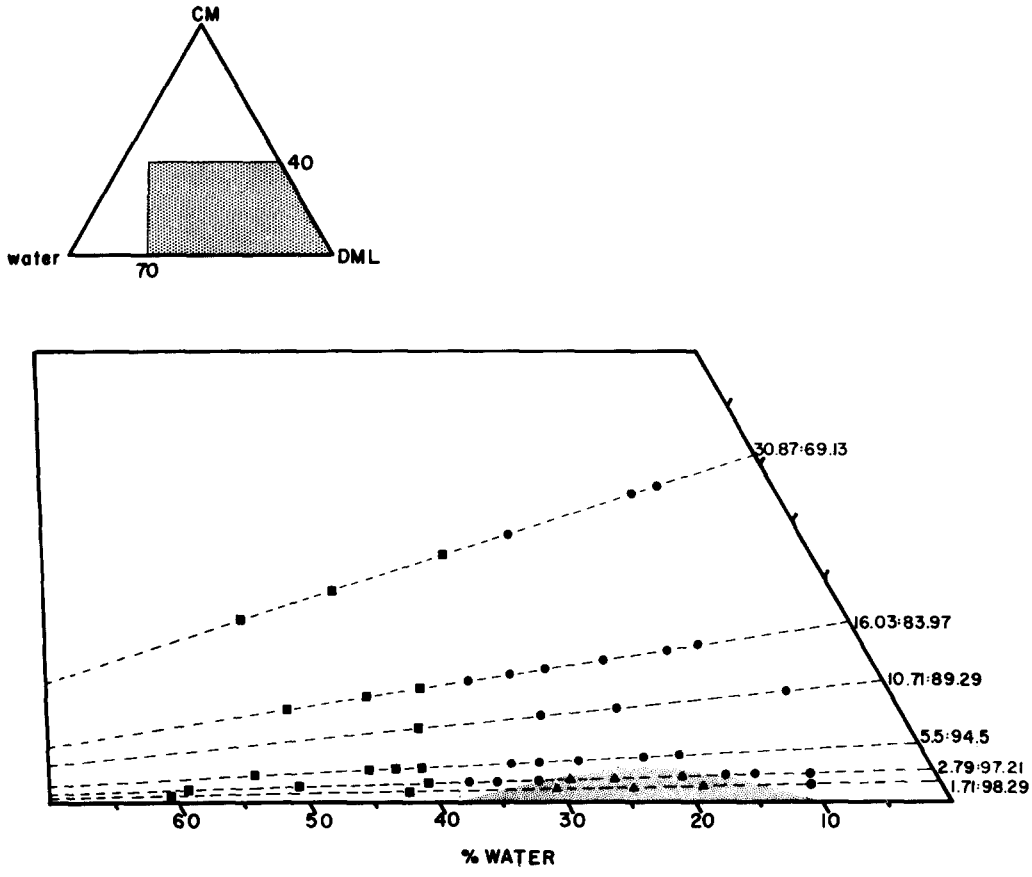


**Fig. 3.** The phases of cholesteryl myristate–dimyristoyl lecithin–water at 37°C. The dotted zone of the triangular coordinate system in (*a*) has been expanded in (*b*). The dashed lines define constant lipid ratios of CM:DML (weight %). (▲) One phase, "neat" textured liquid crystal; (●) two phases, "neat" textured phase and cholesteryl myristate crystals; (■) three phases, "neat" textured phase, cholesteryl myristate crystals and water. The shaded zone in (*b*) approximates the extent of the one phase region.

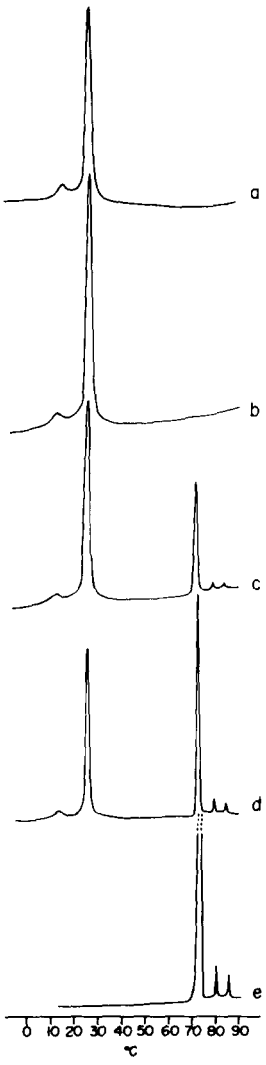


**Fig. 4.** DSC thermograms of mixtures containing DML and CM. (*a*) Hydrated DML containing 35% water; (*b,c,d*) mixtures of CM:DML containing 30% water; (*e*) cholesteryl myristate. Mixtures contain 1.7% CM:98.3% DML (*b*); 10.7% CM:89.3% DML (*c*); 30.9% CM:69.1% DML (*d*).

smectic transition of CM can be detected with 0.01 mg of sample, no detectable transition was observed (sample contained 0.072 mg of CM). In mixtures containing larger amounts of ester (16.0:84.0 and 30.9% CM:69.1% DML), the thermal transitions of DML were similarly unaffected. However, in these mixtures, thermal transitions arising from cholesterol ester were clearly observed (Fig. 4*c* and *d*).

For a series of mixtures containing a constant lipid ratio (e.g., 16.0% CM:84.0% DML) but varying in water content, the observed thermal transitions can be compared to those observed for hydrated DML and cholesteryl myristate. As shown in **Fig. 5**, this series of mixtures exhibits similar hydration dependence as observed for hydrated DML. Both the thermal pretransition and chain-melting transition are observed for mixtures containing CM in the same temperature and hydration range described for DML. The enthalpies of these transitions are unaffected. Similar observations have also been made for mixtures containing 2.8:97.2, 5.5:94.5, 10.7:89.3, and 30.9% CM:69.1% DML. These observations together with the microscopy data indicate that little or no cholesterol ester is associated with the phases of hydrated DML present at temperatures below the chain-melting transition, leaving these thermal transitions unaffected by the presence of cholesterol ester.

In addition to hydrated DML, the thermal transitions arising from cholesteryl myristate were observed and could be correlated with the microscopy results (Fig. 3). No mixtures containing one phase by microscopic observation exhibited thermal transitions associated with cholesteryl myristate, i.e., thermal transitions in the temperature range 70–90°C. For mixtures that exhibited thermal transitions in this temperature range, the transitions were similar to those of CM. In general, for all mixtures examined the crystal to smectic transition temperature, as identified microscopically and observed by DSC, was unchanged. The smectic to cholesteric and cholesteric

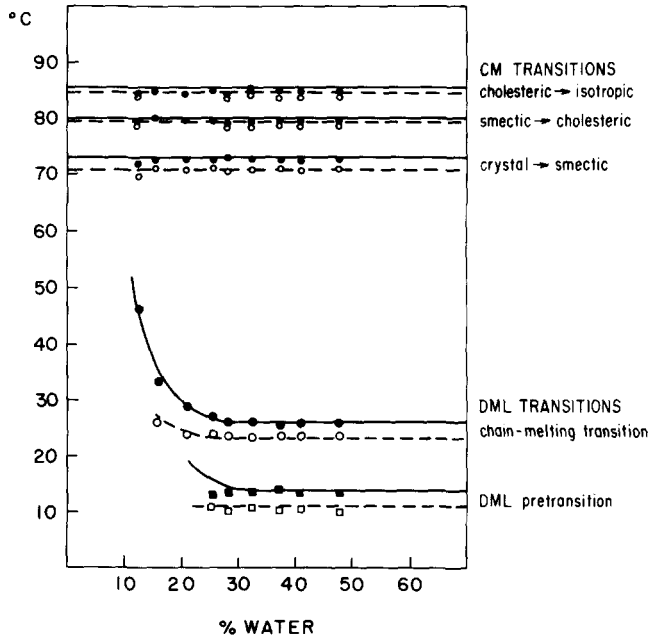


**Fig. 5.** Comparison of thermal transition temperatures observed for mixtures containing 16.0% CM:84.0% DML varying in water content with those found for hydrated DML and cholesteryl myristate. The transition temperatures for hydrated DML are taken from references 17 and 24; the dashed line represents the onset temperature of the transition, the solid line represents endotherm maxima. The hollow symbols represent the onset temperature of the transition observed in the mixtures containing CM and the solid symbols, the endotherm maximum.

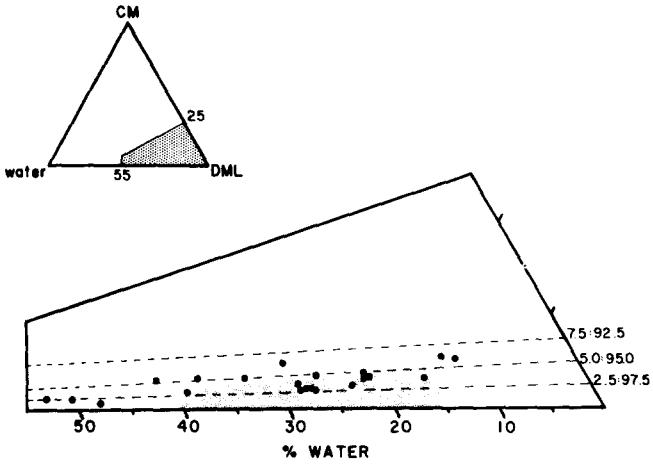


**Fig. 6.** Maximum incorporation of cholesteryl myristate in the liquid crystalline phase of hydrated DML as determined by differential scanning calorimetry. The dotted region of the triangular coordinate system in (*a*) is expanded in (*b*). The dashed lines represent constant lipid ratios of CM:DML. The shaded zone in (*b*) approximates the extent of incorporation of cholesteryl myristate.

to isotropic transition temperatures were ~1°C lower in the ternary mixtures in comparison to CM. However, even in pure cholesterol esters, these liquid crystalline transitions were somewhat variable, suggesting that these minor differences may not be significant.

In contrast to the transition enthalpies associated with DML in the ternary mixtures, the transition enthalpies associated with cholesteryl myristate are not identical to those of CM. In particular, the crystal to smectic transition enthalpy is 30–40% lower than predicted. Since mixtures that are only one phase by microscopy did not exhibit thermal transitions associated with cholesterol ester, it is reasonable to conclude that portions of the cholesterol ester incorporated into the liquid crystalline phase of hydrated DML, $L_\alpha$, do not contribute to the enthalpy of the thermal transitions of CM. Thus, the transition enthalpy is a measure of the "free" or unincorporated cholesteryl myristate that forms an excess phase.

Assuming that the transition enthalpy of the crystal to smectic transition is unchanged ($\Delta H$ = 18.68 cal/g), the fractional part of the total mass of CM present in the sample giving rise to the transition can be determined from the area of the transition endotherm. The remaining amount of CM present in the sample is a measure of the incorporation of cholesteryl myristate into the liquid crystalline phase of DML. From this value, the composition of the mixture in terms of the maximum amount of CM incorporated into the lamellar liquid crystalline phase at ~70°C can be determined. For mixtures containing 10.7:89.3, 16.0:84.0, and 30.9% CM:69.1% DML, the redetermined compositions indicating the extent of incorporation of CM into hydrated DML are plotted in **Fig. 6**. Maximum incorporation of CM occurs between the constant lipid ratios of 2.5:97.5 and 5.0% CM: 94.5% DML. As the water content increases, the amount of cholesterol ester decreases, but even at high water contents, where water is present as an excess phase, some cholesterol ester remains incorporated. These results are consistent with the microscopy observations that suggest increased incorporation of cholesterol ester with increasing temperature.

These conclusions are derived from measurements obtained from the excess phase of cholesteryl myristate at a temperature corresponding to the crystal to smectic transition (70.5°C). However, the microscopy data suggest that the values shown in Fig. 6 are indicative of CM incorporation at lower temperatures, e.g., the equilibration temperature (50–60°C).

### X-ray diffraction

X-ray diffraction patterns were obtained for ternary mixtures containing CM in the same temperature range where the structures $L_{\beta'}$, $P_{\beta'}$, and $L_\alpha$ have been observed for hydrated DML (17). At temperatures below the thermal pretransition and above the chain-melting transition, hydrated DML exhibits several low-angle reflections arising from a one-dimensional lamellar lattice. At temperatures intermediate between the two transitions, several reflections in addition to these lamellar reflections occur and arise from a two-dimensional oblique lattice, $P_{\beta'}$ (**Table 1**). X-ray diffraction patterns obtained for ternary mixtures containing cholesteryl myristate exhibit the same characteristic reflections at a given temperature (see Table 1). In the presence of low amounts of ester, only diffraction patterns associated with the structures of hydrated DML are observed. At higher concentrations of ester, additional reflections associated with CM are also observed.

Similarly the wide-angle diffraction data from mixtures containing cholesteryl myristate can be compared to hydrated DML. The ternary mixtures exhibit the same temperature dependence of the wide-angle x-ray diffraction as hydrated DML in the absence of ester, i.e., at 37°C, a broad diffuse band of intensity centered at (4.6 Å)$^{-1}$; at 20°C, a broad intensity maximum centered at (4.2 Å)$^{-1}$; and at 10°C, a sharp maximum at (4.2 Å)$^{-1}$ together with a broad band at higher values of $s$ (=2 sin $\theta/\lambda$). These x-ray intensity profiles have previously been interpreted (17, 19) as arising from packing variations of the hydrocarbon chains in the $\beta'$ conformation at 10°C and 20°C, or the structure $L_\alpha$ at 37°C.

At 85°C, a diffraction pattern consistent with the

structure $L_\alpha$ is observed (**Fig. 7*a***). At 60°C, a similar diffraction pattern is observed with an additional diffraction maximum present at $s = (33.6\ \text{Å})^{-1}$ (Fig. 7*b*), corresponding to that observed for the smectic phase of CM (Fig. 7*c*). Since homogeneous nucleation of pure CM does not occur above 50°C (15), the presence of the smectic phase at this temperature is not surprising. At 37°C, the crystalline powder diffraction pattern of CM is superimposed on the diffraction observed for the $L_\alpha$ structure (Fig. 7*d*). By comparison with the diffraction pattern for CM (Fig. 7*f*), the contributions to the diffraction pattern from the two phases can be distinguished. Finally at 10°C, the diffraction pattern from $L_{\beta'}$ together with CM is observed (Fig. 7*e*).

In general, mixtures containing ≥5.5% CM exhibited diffraction from the liquid crystalline phase associated with hydrated DML and crystalline cholesteryl myristate. In mixtures containing <5.5% CM, diffraction associated with cholesteryl myristate could not be observed. Thus, the presence of an excess phase of cholesteryl myristate observed by microscopy could not be directly verified by x-ray diffraction at these low ratios.

In the ternary mixtures containing cholesteryl myristate, the structures $L_{\beta'}$, $P_{\beta'}$, and $L_\alpha$ of hydrated DML are observed at the appropriate temperatures. From the microscopy and DSC results, we concluded that below the DML chain-melting transition little or no ester was incorporated into the structures $L_{\beta'}$ and $P_{\beta'}$. Thus, the composition of the diffracting phase in the ternary mixtures is determined only by DML and water and the cholesteryl myristate content can be subtracted from the total composition of the ternary mixture. The corrected composition of the mixtures containing cholesteryl myristate is that of hydrated DML and, for a given water content, the value of the interlamellar repeat, $d$, and cell parameters $a$ and $b$ in the case $P_{\beta'}$ should be equal to the value obtained for the binary system in the absence of CM. For comparison we will refer to the values obtained from the ternary system as $d$(DML + CM) and from the binary system as $d$(DML). In **Table 2**, values of $d$(DML + CM) for mixtures containing variable amounts of cholesteryl myristate (~1–36%) are compared with the values of $d$(DML). After correcting the composition of the ternary mixtures, at a given water content for $L_{\beta'}$ and $P_{\beta'}$, $d$(DML + CM) approximately equals $d$(DML). Further, for the phase $P_{\beta'}$, the cell parameters and indexed reflections are very similar to those of hydrated DML at a similar water content (Table 1). From these results we conclude that there is no incorporation of CM into the $L_{\beta'}$ and $P_{\beta'}$ structures.

The microscopy and DSC results indicate that incorporation of CM occurs at temperatures above the chain-melting transition. From the microscopy data at 37°C, an approximate phase boundary was defined (see Fig. 3). Using this phase boundary, the molar ratio of DML:CM at maximum incorporation can be determined as a function of water content and, for a given ternary mixture, the amount of incorporated cholesterol ester can be obtained. Again, the composition can be corrected and the composition of the diffracting phase determined (see Table 2). The limited incorporation of cholesteryl myristate into the phase $L_\alpha$ does not significantly alter the interlamellar

TABLE 1. Comparison of indexed reflections for mixtures containing (0% CM:100% DML) 28.8% water and (30.87% CM:69.13% DML) 18.7% water at 20°C

| (30.87% CM:69.13% DML) 18% water[a] | | | | (0% CM:100% DML) 28.8% water | |
|---|---|---|---|---|---|
| $S^{-1}$ obs (Å) | $S^{-1}$ calc (Å) | $h$ | $k$ | $S^{-1}$ calc (Å) | $S^{-1}$ obs (Å) |
| 120.2 | 120.2 | 0 | 1 | 121.7 | 121.7 |
| 59.0 | 60.1 | 0 | 2 | 60.8 | 59.4 |
| | 58.9 | 1 | 0 | 59.5 | |
| 50.8[b] | | | | | |
| 39.1 | 39.7 | 1 | 2 | 40.7 | 40.0 |
| | 40.0 | 0 | 3 | 40.5 | |
| 29.4 | 29.4 | 2 | 0 | 29.7 | 29.8 |
| | 29.4 | 2 | $\bar{1}$ | 29.5 | |
| 27.4 | 27.8 | 2 | $\bar{2}$ | 27.8 | 27.9 |
| | 28.0 | 1 | 4 | | |
| 24.8[b] | 25.2 | 2 | $\bar{3}$ | 25.1 | 25.3 |
| 21.7 | 22.0 | 2 | $\bar{4}$ | 22.3 | 22.5 |
| | 21.5 | 1 | 5 | 21.9 | |
| 19.7 | 19.6 | 3 | 0 | 19.8 | 19.9 |
| | 19.7 | 3 | $\bar{1}$ | 19.8 | |
| 18.5 | 18.0 | 3 | 2 | 18.4 | 18.1 |
| | 18.6 | 3 | $\bar{3}$ | 18.5 | |
| 17.4 | 17.4 | 3 | $\bar{4}$ | 17.3 | 17.0 |
| 16.0 | 15.6 | 3 | 4 | | |
| | 16.2 | 3 | $\bar{5}$ | | |
| 14.8 | 14.7 | 4 | 0 | 14.9 | 14.9 |
| | 14.8 | 4 | $\bar{1}$ | 14.9 | |
| 13.8 | 13.4 | 4 | $\bar{5}$ | | |
| 12.8 | 12.6 | 4 | 4 | | |
| 11.8 | 11.8 | 5 | 0 | 11.9 | 11.9 |
| | 11.9 | 5 | $\bar{1}$ | 11.9 | |
| $a$ = 59.3 Å | | | | $a$ = 60.1 Å | |
| $b$ = 121.1 Å | | | | $b$ = 121.6 Å | |
| $\gamma$ = 95 deg. | | | | $\gamma$ = 95 deg. | |

[a] Subtracting the cholesteryl myristate content from this mixture and correcting the composition of (0% CM:100% DML) 26.2% water.

[b] The observed reflection at 50.8 Å corresponds to the 002 reflection of CM; the 004 reflection overlaps with the 2-3 reflection from $P_{\beta'}$.

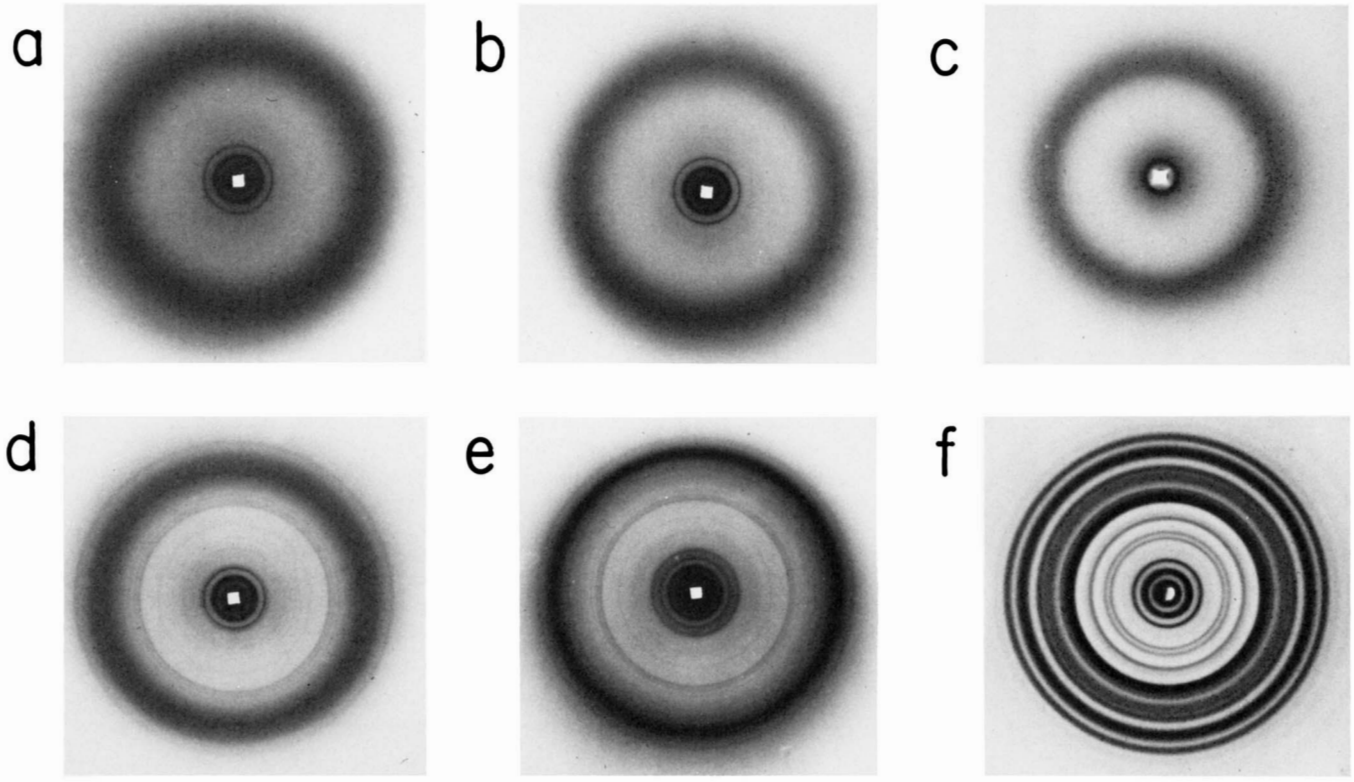


**Fig. 7.** X-ray diffraction patterns obtained for a mixture containing 31.8% water (5.5% CM:94.5% DML) at 85°C (*a*), 60°C (*b*), 37°C (*d*), 10°C (*e*), and cholesteryl myristate at 74°C (*c*) and 37°C (*f*).

repeat, *d* (DML + CM) ~ = *d*(DML). This observation is discussed in detail below.

### Structural effects of incorporation

Model electron density distributions for the CM–DML bilayer structure were determined for different orientations of the ester and the calculated continuous Fourier transforms were compared with the DML bilayer structure model. The bilayer structure was assumed to contain 5 wt% cholesterol ester (molar ratio DML:CM = 15.1), an upper limit of incorporation. Three orientations of cholesterol ester are considered

TABLE 2. Comparison of interlamellar repeat for hydrated mixtures containing cholesteryl myristate, *d*(DML + CM), and hydrated dimyristoyl lecithin, *d*(DML), at 10, 20, and 37°C

| | | | $L_{\beta'}$ (10°C)[a] | | | $P_{\beta'}$ (20°C)[a] | | $L_\alpha$ (37°C)[b] | | | |
|---|---|---|---|---|---|---|---|---|---|---|---|
| %CM | %DML | $\%H_2O$ | $\%H_2O$[a] | *d*(DML + CM) | *d*(DML) | *d*(DML + CM) | *d*(DML) | molar ratio DML:CM | $\%H_2O$[b] | *d*(DML + CM) | *d*(DML) |
| 9.10 | 75.90 | 15.00 | 16.50 | 53.7 Å | 53.1 Å | 53.6 Å[c] | 53.4 Å[c] | 36:1 | 16.15 | 48.3 Å | 48.1 Å |
| 29.45 | 57.93 | 12.62 | 17.89 | 54.2 | 53.7 | | | 34:1 | 17.37 | 48.1 | 48.1 |
| 4.44 | 76.36 | 19.20 | 20.09 | 53.9 | 54.1 | 54.0[c] | 54.2[c] | 25:1 | 19.54 | 48.2 | 48.1 |
| 4.29 | 73.71 | 22.00 | 22.99 | 56.5 | 55.7 | | | 20:1 | 22.22 | 48.0 | 48.3 |
| 8.28 | 69.02 | 22.70 | 24.74 | 57.3 | 57.0 | 55.9 | 56.2 | 20:1 | 23.91 | 49.6 | 48.5 |
| 8.15 | 67.94 | 23.91 | 26.03 | 59.3 | 58.0 | 58.7 | 58.9 | 21:1 | 25.21 | 49.2 | 48.7 |
| 36.08 | 45.92 | 18.00 | 28.16 | 58.0 | 59.5 | 59.0 | 59.3 | 24:1 | 27.06 | 49.9 | 49.3 |
| 3.95 | 67.85 | 28.21 | 29.37 | 59.6 | 60.4 | | | 25:1 | 28.65 | 51.3 | 50.4 |
| 1.19 | 68.47 | 30.34 | 30.71 | 60.6 | 61.7 | 61.0 | 61.5 | 50:1[d] | 30.34 | 52.5 | 51.3 |
| 3.84 | 65.96 | 30.20 | 31.40 | 61.0 | 61.7 | | | 31:1 | 30.79 | 51.5 | 51.5 |
| 6.87 | 57.22 | 35.91 | 38.56 | 60.9 | 61.7 | 64.7 | 64.8 | 270:1 | 38.48 | 58.0 | 58.2 |
| 6.42 | 53.48 | 40.11 | 42.86 | 61.5 | 61.7 | 64.7 | 64.8 | [e] | 42.86 | 60.9 | 59.7 |
| 15.39 | 30.29 | 54.31 | 64.19 | | | | | [e] | 64.19 | 60.3 | 59.7 |

[a] At 10 and 20°C, the composition of the ternary mixtures is corrected assuming no ester is incorporated.
[b] At 37°C, the composition of the ternary mixtures is corrected assuming incorporation of CM occurs, the degree of incorporation (molar ratio DML:CM) determined from the microscopy results at 37°C.
[c] Mixtures that exhibited the phase $L_{\beta'}$ at 20°C.
[d] Does not represent maximum incorporation.
[e] No cholesteryl myristate incorporated.

(see **Fig. 8**). The recent crystal structure determination of cholesteryl myristate by Craven and DeTitta (20) has provided structural data for the calculation of these model distributions. In model I, the cholesterol ester is in a "kinked" molecular geometry with both the myristate chain and the steroid ring located perpendicular to the bilayer plane and roughly parallel to the phospholipid molecule. Only the ester linkage protrudes into the polar region. In model II, cholesteryl myristate is "extended perpendicular" to the bilayer plane, again roughly parallel to the phospholipid molecules. In model III, CM is oriented "extended perpendicular" to the long axis of the phospholipid and located in the center of the bilayer. The transforms obtained for the three models and variations on each model are superimposable on that observed for hydrated DML (the details of these calculations and the Fourier transforms are given in the Appendix). Thus, with this limited incorporation of CM, analysis of the x-ray diffraction data does not yield any direct information on the molecular geometry of cholesterol ester in the phospholipid bilayer. However, some general features of cholesterol ester–phospholipid interactions are apparent. In Table 2, we have shown that the interlamellar repeat of the mixed lipid system at maximum incorporation is nearly identical to that observed for hydrated DML at the same water content. The same is true for the bilayer thickness, $d_1$, and the surface area per lipid molecule $S_1$ (see **Table 3**). However, the number of molecules per unit surface area, $N_1$ is on the average ~1% higher in the mixed lipid system compared to DML. This is in contrast to that observed for cholesteryl linolenate–egg lecithin–water (10) and suggests that, if cholesteryl myristate is located at the lipid–water interface, a molecular geometry occupying a surface area less than that of DML might be favored.

We can further examine the three models (Fig. 8) by calculating the surface area of DML in the mixed lipid system. From the molecular volumes and lengths calculated from CM (see Appendix), the calculated surface area for the cholesterol moiety is 40.8 Å² and that of the myristate chain is 28.2 Å². Assuming all the cholesteryl myristate is at the surface for model I (kinked), the surface area of cholesterol ester is $S$(CM) = 79 Å² and for model II (extended perpendicular), $S$(CM) = 40.8 Å². In model III (extended parallel) $S$(CM) = 0, since no cholesterol ester is assumed to be at the surface. As shown in Table 3, the calculated values of $S$(DML) for the three models are similar, with the largest deviation from the value of hydrated DML occurring for model III. Furthermore, the small differences in the values obtained are insufficient to distinguish between models I and II.

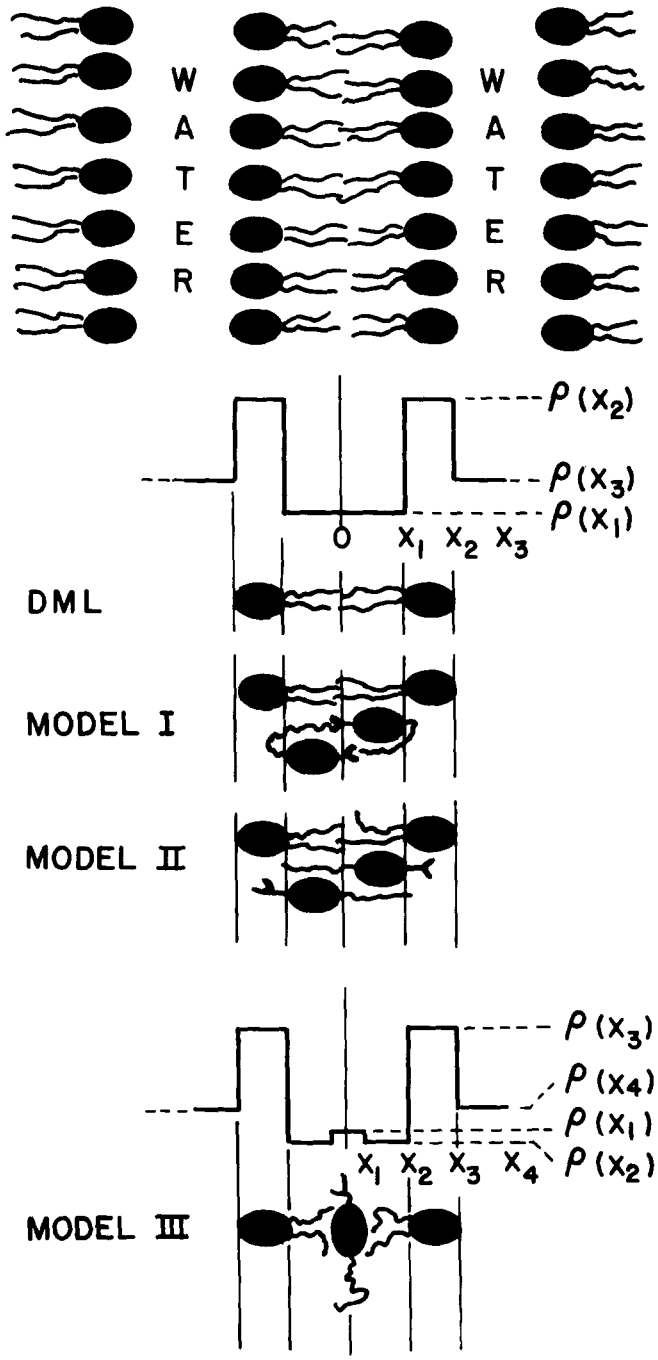


**Fig. 8.** Three generalized molecular orientations of cholesteryl myristate incorporated in the DML bilayer structure. In model I, CM assumes a "kinked" molecular geometry; in model II, "extended perpendicular" to the bilayer plane; model III "extended parallel" to the bilayer plane. The details of the calculation and assigned values of $x$ and $\rho$ ($x$) are given in the Appendix.

Thus, in contrast to the cholesteryl linolenate–egg lecithin–water system, the differences in the structural parameters found for cholesteryl myristate–dimyristoyl lecithin–water are very small, perhaps due to similarities in the molecular lengths of the two lipid components.

TABLE 3. Experimental and calculated molecular parameters for the structure $L_\alpha$ of hydrated dimyristoyl lecithin and the mixed lipid system of cholesteryl myristate–dimyristoyl lecithin–water at maximum incorporation of ester

| %Water | DML/CM | $d$(DML) | $d$(DML + CM) | $d_1$(DML) | $d_1$(DML + CM) | $S_1$(DML) | $S_1$(DML + CM) | $S'_1$(DML) | $S'_{II}$(DML) | $S'_{III}$(DML) |
|---|---|---|---|---|---|---|---|---|---|---|
| 16.15 | 36/1 | 48.1 Å | 48.3 Å | 40.2 Å | 40.4 Å | 54.1 Å² | 54.8 Å² | 55.8 Å² | 54.7 Å² | 55.8 Å² |
| 17.37 | 34/1 | 48.1 | 48.1 | 39.6 | 39.6 | 56.0 | 55.9 | 56.7 | 55.9 | 57.5 |
| 19.54 | 25/1 | 48.1 | 48.2 | 38.5 | 38.6 | 57.6 | 57.3 | 58.4 | 56.9 | 59.6 |
| 22.22 | 20/1 | 48.3 | 48.0 | 37.4 | 37.2 | 59.3 | 59.5 | 60.2 | 58.4 | 63.5 |
| 23.91 | 20/1 | 48.5 | 49.6 | 36.8 | 37.7 | 60.2 | 58.7 | 61.1 | 59.3 | 61.6 |
| 25.21 | 21/1 | 48.7 | 49.2 | 36.3 | 36.7 | 61.0 | 60.3 | 61.8 | 60.1 | 63.2 |
| 27.06 | 24/1 | 49.3 | 49.9 | 35.8 | 36.3 | 61.9 | 61.0 | 62.5 | 61.0 | 63.5 |
| 28.65 | 25/1 | 50.4 | 51.3 | 35.8 | 36.5 | 61.9 | 60.6 | 62.6 | 61.1 | 63.0 |
| 30.20 | 31/1 | 51.5 | 51.5 | 35.5 | 35.5 | 62.4 | 62.4 | 61.8 | 61.0 | 62.0 |
| 38.48 | 270/1 | 58.2 | 58.0 | 35.6 | 35.4 | 62.2 | 62.6 | 62.6 | 62.6 | 62.6 |
| 42.86 | [a] | 59.7 | 60.9 | 35.6 | 36.0 | 62.2 | 61.6 | 61.6 | 61.6 | 61.6 |
| 64.19 | [a] | 59.7 | 60.3 | 35.6 | 35.9 | 62.2 | 61.7 | 61.7 | 61.7 | 61.7 |

For hydrated DML, $d$(DML) is the interlamellar repeat distance, $d_1$(DML) is the bilayer thickness, and $S_1$(DML) is the mean molecular area. For the mixed lipid system, $d$(DML + CM) is the interlamellar repeat distance, $d_1$(DML + CM) is the bilayer thickness, and $S_1$(DML + CM) is the mean molecular area. $S'_1$(DML) is calculated assuming all the cholesteryl myristate is at the interface and occupies an area of 79 Å². $S'_{II}$(DML) is calculated assuming all the cholesterol ester is at the interface and occupies an area of 40.8 Å². $S'_{III}$(DML) is calculated assuming no cholesterol ester is at the interface.

[a] No cholesterol ester incorporated.

## DISCUSSION

### Cholesteryl myristate–dimyristoyl lecithin–water

Hydrated dimyristoyl lecithin undergoes two thermal transitions in the temperature range 0–90°C, a thermal pretransition at 11°C (at water concentrations ≥20%), and the chain-melting transitions at 23°C (at all water contents ≥20%; this transition occurs at higher temperatures at <20% water). At temperatures below the thermal pretransition, hydrated dimyristoyl lecithin forms the structure $L_{\beta'}$. The pretransition is associated with the formation of the structure $P_{\beta'}$. At the chain-melting transition a lamellar liquid crystalline structure, $L_\alpha$, forms.

Cholesteryl myristate does not interact with dimyristoyl lecithin below the chain-melting transition in either the $L_{\beta'}$ or $P_{\beta'}$ phase. In the $L_\alpha$ phase only limited but variable incorporation of cholesterol ester occurs depending on the temperature, higher amounts of ester being incorporated at higher temperatures. Maximum incorporation of ester into the phase $L_\alpha$ also varies with the degree of hydration. Polarizing light microscopy results at 37°C indicate that the approximate limiting molar ratio of CM:DML increases from 1:36 to 1:20 upon increasing the water concentration from 16 to 22% (w/w). Between 22 and 25% water, the CM:DML ratio remains at ~1:20. At higher water concentrations, a progressive decrease in the ester content occurs until essentially no cholesteryl myristate remains incorporated at maximum hydration of dimyristoyl lecithin (40% water). The DSC results indicate that increased amounts of cholesterol ester are incorporated into the $L_\alpha$ phase at higher temperatures, e.g., 70.5°C. Although it is not clear how the incorporation of CM changes between 23 and 70.5°C, we will assume that, at the sample equilibration temperature (50–60°C), the sample composition is similar to that at 70.5°C. In addition, DSC shows that at water contents between 15 and 25% (w/w) the limiting molar ratio of CM:DML in the phase $L_\alpha$ is 1:17. Increasing the water content results in a progressive decrease in the limiting molar ratio to 1:26 at 40% water. The lamellar phase is the only phase (except at low water contents, <5%) in which all three components mutually interact. All mixtures of the three components having compositions outside the one-phase zone produce additional phases of cholesteryl myristate or water, or both.

Using model electron density distributions, x-ray diffraction analysis could not differentiate between the mixed lipid system and DML–water in the absence of ester, due to the limited incorporation of cholesteryl myristate (see Appendix). Calculated structural parameters for this mixed lipid system are nearly identical to DML–water in the absence of ester and are consistent with strong similarities in the molecular parameters of cholesteryl myristate and dimyristoyl lecithin.

### Interrelationships in cholesterol ester–phospholipid systems

This study, together with the cholesteryl linolenate–egg lecithin–water (10) and cholesteryl linoleate–egg lecithin–water (21) systems, allows for comparison of three different cholesterol ester–phospholipid–water systems, the cholesterol esters varying in chain length or degree of unsaturation. Plotted in **Fig. 9** is a comparison of maximum incorporation of cholesterol ester into the $L_\alpha$ phase of DML as a function of hydration. For both cholesteryl lin-

olenate–egg lecithin–water ($C_{18:3}$ system) and cholesteryl linoleate–egg lecithin–water ($C_{18:2}$ system) the data shown are at 23°C. In these mixed lipid systems, the chain-melting transition of hydrated egg lecithin (−7°C) is unaffected by the presence of cholesterol ester. Relative to this transition these studies were carried out at a temperature 30°C higher (T + 30). For cholesteryl myristate–dimyristoyl lecithin–water ($C_{14:0}$ system), the results are presented at 37°C (T + 14) as determined from the microscopy data and at ~T + 35°C as determined from DSC.[3] In order to compare these systems directly, the data in Fig. 9 are plotted as the molar ratio of cholesterol ester to phospholipid (CE:PL) on the ordinate and the molar ratio of water to total lipid (cholesterol ester + phospholipid) on the abscissa.

The $C_{14:0}$ system (at T + 14) and the $C_{18:2}$ (T + 30) system exhibit very similar behavior over all hydration values, both systems incorporating no cholesterol ester at a water:lipid ratio of 28:1. The somewhat higher values of CE:PL for the $C_{18:2}$ system may be a temperature effect; the results for this system were obtained at a higher temperature relative to the chain-melting temperature of each lecithin (T + 30 for the $C_{18:2}$ system and T + 14 for the $C_{14:0}$ system). This observation would indicate that the temperature-induced disorder allows for increased incorporation of cholesterol ester. The increased incorporation of cholesteryl myristate in the $C_{14:0}$ system at higher temperature supports this observation, as does the increased incorporation of cholesteryl linolenate in the high-temperature phases of anhydrous egg lecithin (22).

Incorporation of cholesterol ester in the $C_{18:3}$ system exhibits a different hydration dependence. Although the molar ratios of CE:PL are quantitatively different, the $C_{18:3}$ system exhibits similar hydration dependence to that of the $C_{14:0}$ system at higher temperature (T + 35), above a water:lipid ratio of 8:1. At a water:lipid ratio of ~28:1, both systems incorporate comparable amounts of cholesterol ester (CE:PL 1:30). This observation suggests that the degree of unsaturation may be equivalent to that of thermal disordering.

To probe further the significance of chain unsaturation of cholesterol ester, the structural parameters for the $C_{18:2}$ and $C_{18:3}$ systems at the same temperature are compared (23°C, i.e., T + 30). Although the molecular orientation of cholesterol ester in the phospholipid bilayer could not be determined, the data were more consistent with the molecular axis of cholesterol ester being oriented perpendicular to the plane of the

[3] The degree of incorporation of CM at the equilibration temperature of 50–60°C (i.e., ~T + 35°C) is assumed to be similar to that recorded at 70.5°C by DSC (see Results).

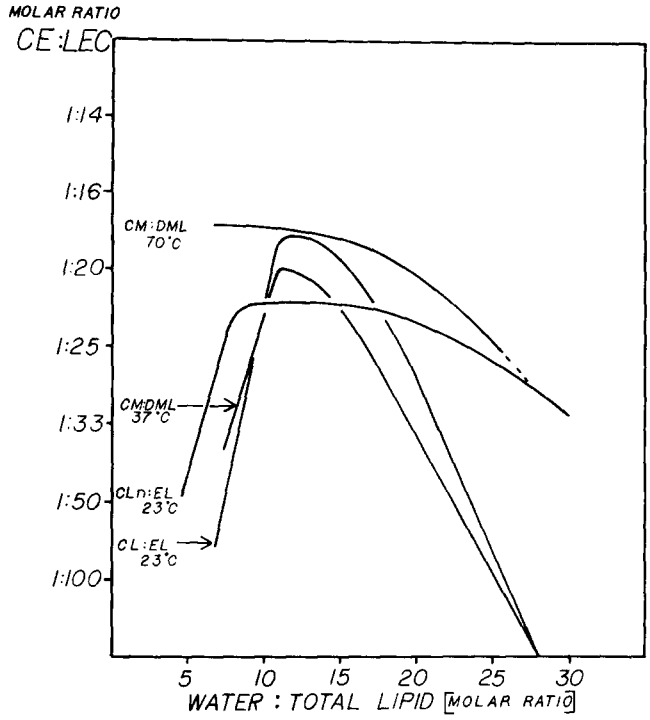


**Fig. 9.** Incorporation of cholesterol ester in the liquid crystalline phase of phospholipid as a function of hydration. 14:0, Cholesteryl myristate–dimyristoyl lecithin–water at 37°C (T + 14) and at T + 35; 18:2, cholesteryl linoleate–egg lecithin–water at 23°C (T + 30), data from reference 21; 18:3, cholesteryl linolenate–egg lecithin–water at 23°C (T + 30), data from reference 10. T corresponds to the chain-melting transition temperature of each lecithin.

bilayer. Regardless of the orientation, incorporation of cholesterol ester could affect the mean molecular surface area calculated from the x-ray diffraction data either indirectly by being located entirely in the apolar region of the phospholipid bilayer, or directly by being located at the lipid–water interface. These effects will be reflected in the average number of lipid molecules per unit surface area, $N_1$. By comparison of this value for the mixed lipid system, $N_1$(CE + PL), with the values obtained for lecithin alone, $N_1$(PL), the net difference $\Delta N_1$ can be calculated for the $C_{18:2}$ system and $C_{18:3}$ system at the same temperature. A negative difference indicates that fewer molecules per unit surface area are present as compared with lecithin–water in the absence of cholesterol ester. This net difference in molecules per unit surface area is shown in **Figure 10** for the $C_{18:2}$ system and $C_{18:3}$ system. Both systems show a negative deviation, the $C_{18:2}$ system by a maximum of only ~3%. This further suggests a disordering effect related to the degree of unsaturation of the cholesterol ester.

The significance of these deviations can be examined utilizing the calculated structural parameters $d_1$ and $S_1$. Assuming the values of these parameters were obtained for lecithin–water in the absence of

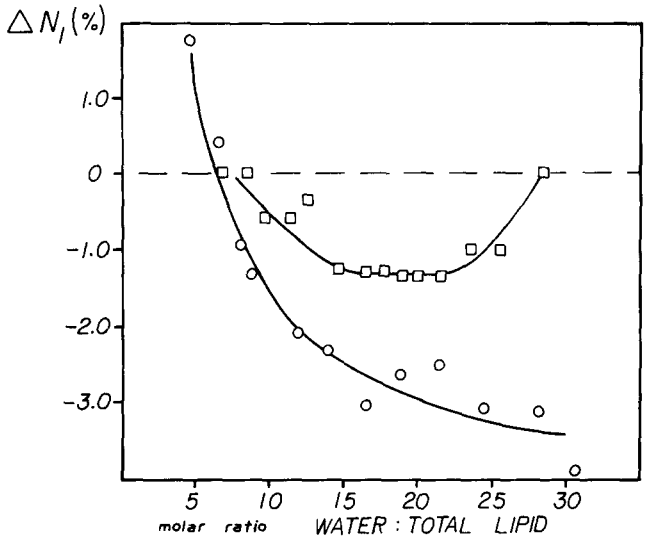


**Fig. 10.** The net difference in the number of molecules per unit surface area $\Delta N_1$. $N_1$(PL) is the number of molecules occupying the surface of the pure phospholipid system and is compared to that of the mixed lipid system $N_1$(CE + PL) where $\Delta N_1 = N_1(PL) - N_1(CE + PL)/N_1(PL)$. (○) Cholesteryl linolenate–egg lecithin–water at 23°C; (□) cholesteryl linoleate–egg lecithin–water at 23°C. The values for cholesteryl linoleate are from reference 21 and for cholesteryl linolenate from reference 10.

cholesterol ester, the temperature at which these parameters would be observed for lecithin–water alone may also be calculated. The surface areas obtained for the $C_{18:2}$ system are essentially the same as would be obtained for egg lecithin–water at 23°C (T + 30°C). For the $C_{18:3}$ system, the calculated values of surface areas for this mixed lipid system at T + 30°C are the same as would be obtained for egg lecithin alone at T + 34°C. These calculations suggest that for the $C_{18:2}$ system the small differences in $\Delta N_1$ are probably not as significant as those found for the $C_{18:3}$ system.

These observations suggest the following regarding the interactions of cholesterol ester with phospholipids: *1*) the incorporation of cholesterol ester is a temperature-dependent phenomenon requiring the existence of a thermally disordered liquid crystalline structure; *2*) the extent of incorporation is also temperature dependent; increasing amounts of cholesterol ester can be incorporated at higher temperatures relative to the chain-melting transition; *3*) the structural effect of thermal disordering of phospholipid bilayers (bilayer thickness, surface area, etc.) may also be induced by the presence of highly unsaturated cholesterol esters. Although this effect is not readily apparent for the *cis* di-unsaturated ester, cholesteryl linoleate, it is observed for cholesteryl linolenate (*cis,cis,cis* Δ9,12,15-octadecatrienoate). Similar behavior may also occur for other highly unsaturated cholesterol esters.

## Biological relevance

Biological membranes appear to contain little or no cholesterol ester. Recently, Zambrano, Fleischer, and Fleischer (23) measured the lipid content of specific rat liver subcellular fractions. Expressed in terms of weight percent cholesterol ester (based on CE + PL only), values in the range of 1.3 to 3.7% were found. The amount of cholesterol ester based on either total lipid or only CE + PL content is comparable to that determined in the model cholesterol ester–phospholipid systems described here, especially when the marked heterogeneity of lipids present in these subcellular fractions is considered. These observations strongly suggest that the limited presence of cholesterol esters in membrane systems is explained in terms of simple lipid–lipid interactions.

The authors wish to acknowledge helpful discussions with Dr. C. R. Loomis. This research was supported by U. S. Public Health Service grants HL18623, GM00176, and HL07291.

*Manuscript received 30 January 1978; accepted 24 July, 1978.*

## REFERENCES

1. Eisenberg, S., and R. I. Levy. 1975. Lipoprotein metabolism. *Adv. Lipid Res.* **13:** 1–89.
2. Riley, C. 1963. Lipids of human adrenals. *Biochem. J.* **89:** 500–507.
3. Stewart, G. T. 1961. Mesomorphic forms of lipid in the structure of normal and athermomatous tissues. *J. Pathol. Bacteriol.* **81:** 385–393.
4. Smith, E. B. 1965. The influence of age and atherosclerosis on the chemistry of aortic intima. Part I. The lipids. *J. Atheroscler. Res.* **5:** 224–240.
5. Bottcher, C. J. F., and C. M. Van Gent. 1961. Changes in the composition of phospholipids and phospholipid fatty acids associated with atherosclerosis in the human aortic wall. *J. Atheroscler. Res.* **1:** 36–46.
6. Smith, E. B., P. H. Evans, and M. D. Downham. 1967. Lipid in the aortic intima. The correlation of morphological and chemical characteristics. *J. Atheroscler. Res.* **7:**171–186.
7. Smith, E. B., and R. S. Slater. 1972. The microdissection of large atherosclerotic plaques to give morphologically and topographically defined fractions for analysis. Part I. The lipids in the isolated fractions. *Atherosclerosis.* **15:** 37–56.
8. Small, D. M., and G. G. Shipley. 1974. Physical-chemical basis of lipid deposition in atherosclerosis. *Science.* **185:** 222–229.
9. Katz, S. S., G. G. Shipley, and D. M. Small. 1976. Physical chemistry of the lipids of human atherosclerotic lesions. Demonstrations of a lesion intermediate between fatty streaks and advanced plaques. *J. Clin. Invest.* **58:** 200–211.
10. Janiak, M. J., C. R. Loomis, G. G. Shipley, and D. M. Small. 1974. The ternary phase diagram of lecithin,

cholesteryl linolenate and water: Phase behavior and structure. *J. Mol. Biol.* **86:** 325–329.
11. Chadha, J. S. 1970. Preparation of crystalline L-α-glycerophosphoryl choline–cadmium chloride adduct from commercial egg lecithin. *Chem. Phys. Lipids.* **4:** 104–108.
12. Cubero Robles, E., and D. Van Den Berg. 1969. Synthesis of lecithins by acylation of *O*-(*sn*-glycero-3-phosphoryl) choline with fatty acid anhydrides. *Biochim. Biophys. Acta.* **187:** 520–526.
13. Franks, A. 1955. An optically focusing x-ray diffraction camera. *Proc. Phys. Soc. (London) Sect. B.* **68:** 1054–1064.
14. Elliott, A. 1965. The use of toroidal reflecting surfaces in x-ray diffraction cameras. *J. Sci. Instrum.* **42:** 312–316.
15. Price, F. P., and J. H. Wendorff. 1971. Transitions in mesophase forming systems. I. Transformation kinetics and pretransition effects in cholesteryl myristate. *J. Phys. Chem.* **75:** 2839–2853.
16. Barrall, E. M., R. S. Porter, and J. F. Johnson. 1967. The polymorphism of cholesteryl esters: Differential thermal and microscopic measurements on cholesteryl myristate. *Mol. Cryst.* **3:** 103–115.
17. Janiak, M. J., D. M. Small, and G. G. Shipley. 1976. Nature of the thermal pretransition of synthetic phospholipids: Dimyristoyl and dipalmitoyl lecithin. *Biochemistry.* **15:** 4575–4580.
18. Rosevear, F. 1954. The microscopy of the liquid crystalline neat and middle phases of soaps and synthetic detergents. *J. Am. Oil Chem. Soc.* **31:** 628–639.
19. Tardieu, A., V. Luzzati, and F. C. Reman. 1973. Structure and polymorphism of the hydrocarbon chains of lipids: A study of lecithin–water phases. *J. Mol. Biol.* **75:** 711–733.
20. Craven, B. M., and G. T. DeTitta. 1976. Cholesteryl myristate: Structures of the crystalline solid and mesophases. *J. Chem. Soc. (Perkin Trans. II).* 814–822.
21. Loomis, C. R. 1977. The physical interactions of cholesterol esters, cholesterol and phosphatidylcholine. Ph.D. Thesis, Boston University, Boston, MA.
22. Loomis, C. R., M. J. Janiak, D. M. Small, and G. G. Shipley. 1974. The binary phase diagram of lecithin and cholesteryl linolenate. *J. Mol. Biol.* **86:** 309–324.
23. Zambrano, F., S. Fleischer, and B. Fleischer. 1975. Lipid composition of the Golgi apparatus of rat kidney and liver in comparison with other subcellular organelles. *Biochim. Biophys. Acta.* **380:** 357–369.
24. Janiak, M. J. 1977. The structure of phosphatidylcholines and their interaction with cholesterol ester. Ph.D. Thesis, Boston University, Boston, MA.

## APPENDIX I

### CALCULATION OF MODEL ELECTRON DENSITY DISTRIBUTION FOR CHOLESTEROL MYRISTATE–DIMYRISTOYL LECITHIN BILAYERS

Model electron density distributions were calculated assuming 3- and 4-level square well models (including solvent).

The electron content and molecular volume of dimyristoyl lecithin was determined from the partial specific volume ($\bar{v}_l = 0.983$ at 37°C),[1] the molecular weight (M = 678), and the number of electrons ($n = 374$). Using the values obtained by Reiss-Husson and Luzzati (A1), the average volume of the hydrocarbon chains in the liquid-like conformation was determined and, by difference, the volume of the polar head group. From these values the electron densities of the hydrocarbon chain and polar head group region were calculated (**Table A-1**). The electron density of the water layer was assumed to be 0.334. The width of each level was calculated from the interlamellar repeat value obtained for hydrated DML (~30% water).

To obtain electron density values for cholesteryl myris-

[1] Laggner, P., and H. Stabinger, unpublished observations.

TABLE A-1. Calculation of electron density for hydrated dimyristoyl lecithin and cholesterol myristate

| DML Hydrocarbon Chains | $-CH_2-$ | $-CH_3$ | DML Polar Head Group | |
|---|---|---|---|---|
| Number of groups | 24 | 2 | Number of electrons | 164 |
| Number of electrons/group | 14 | 15 | Volume (by difference) ($V_{total} - V_{chains}$ = 1105 − 755.5) (Å³) | 349.5 |
| Volume/group (Å³) | 27 | 54 | | |
| Total volume | 755.5 | | | |
| Total electron content | 210 | | | |

| Hydrated Dimyristoyl Lecithin | | Hydrocarbon Chains | Polar Head Group | Water |
|---|---|---|---|---|
| Average volume | $\bar{V}$(Å³) | 755.5 | 349.5 | |
| Electron content | $\bar{n}(e^-)$ | 210 | 164 | |
| Electron density | ($e^-$/Å³) | 0.278 | 0.468 | 0.334 |
| Length | $x$(Å) | 9.9 | 8.0 | 8.35 |

| Cholesteryl Myristate | | Side Chain | Steroid Nucleus | Ester Linkage | Hydrocarbon Chain |
|---|---|---|---|---|---|
| Formula weight | $\bar{M}$ | 113 | 257 | 227 | 183 |
| Average volume | $\bar{V}$(Å³) | 284 | 361.6 | 51.2 | 377.8 |
| Electron content | $\bar{n}(e^-)$ | 65 | 142 | 22 | 105 |
| Electron density | ($e^-$/Å³) | 0.229 | 0.393 | 0.429 | 0.278 |
| Length | Å | 6.75 | 8.86 | 2.32 | 9.9 |

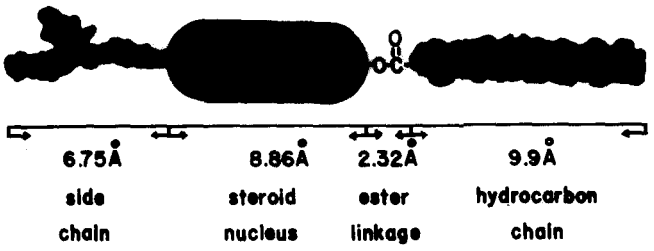


**Fig. A-1.** Schematic representation of the cholesteryl myristate molecule showing the lengths assigned to the side-chain, steroid nucleus, ester linkage, and hydrocarbon chain regions.

tate, the data of Craven and DeTitta (A2) were used. The volume of the steroid nucleus was obtained from the partial densities: $\bar{v}_1$ (side chain) = 0.75, $\bar{v}_1$ (steroid nucleus) = 1.18, $\bar{v}_1$ (fatty acid) = 1.02. To obtain the volume of the ester linkage, the subcell parameters of the myristate chains were utilized to determine the volume of the hydrocarbon chain and, by difference, the volume of the ester linkage: $V$ (fatty acid) $-$ $V$ (hydrocarbon chain not including ester group). The volume of the side chain in the melted state was assumed to be the same as for cholesterol (see reference A3). The volume of the hydrocarbon chain of the ester was assumed to be the same as that for the phospholipid. Thus, the cholesteryl myristate molecule was divided into four segments: the side chain, steroid nucleus, ester linkage, and hydrocarbon chain. The length of the steroid nucleus and ester linkage was determined from the crystal structure by projection onto the molecular axis. The values of molecular length and electron density are summarized in **Fig. A-1** and Table A-1, respectively.

Three generalized models of molecular orientation of cholesteryl myristate incorporated into the bilayer structure of hydrated DML were considered (see Fig. 8 above). Model I assumes that 100% of the CM side chain, steroid nucleus, and hydrocarbon chain are located in the hydrocarbon region of DML and 100% of the ester linkage is in the polar region. A variation on Model I also tested assumes that 100% of the CM side chain and hydrocarbon chain and 65% of the steroid nucleus are located in the hydrocarbon region of DML, and that 35% of the steroid nucleus and 100% of the ester linkage are located in the polar region.

Model II assumes that 100% of the steroid side chain and 14% of the steroid nucleus reside in the polar region and 86% of the steroid nucleus and 77% of the hydrocarbon chain of CM reside in the hydrocarbon region of DML. An extra level located near the center of the bilayer exists and

TABLE A-2. Contributions of molecular components to electron density of various electron density levels of hydrated dimyristoyl lecithin bilayer structure

| | %$T$ | $\bar{n}(e^-)$ | $\bar{V}$(Å$^3$) | $\kappa$ | $\bar{n}_\kappa(e^-)$ | $\bar{V}_\kappa$(Å$^3$) | %$T$ | $\bar{n}(e^-)$ | $\bar{V}$(Å$^3$) | $\kappa$ | $\bar{n}_\kappa(e^-)$ | $\bar{V}_\kappa$(Å$^3$) |
|---|---|---|---|---|---|---|---|---|---|---|---|---|
| | DML | | | | | | DML:CM Model I | | | | | |
| DML Hydrocarbon Region | | | | | | | | | | | | |
| DML Hydrocarbon Chain | 100 | 210 | 755.5 | 1.0 | 210 | 755.5 | 100 | 210 | 755.5 | 0.933 | 196 | 705.1 |
| CM Steroid Side Chain | | | | | | | 100 | 65 | 284 | 0.067 | 4.3 | 18.9 |
| CM Steroid Nucleus | | | | | | | 100 | 142 | 361.6 | 0.067 | 9.5 | 24.2 |
| CM Ester Linkage | | | | | | | 0 | | | | | |
| CM Hydrocarbon Chains | | | | | | | 100 | 105 | 377.8 | 0.067 | 7.0 | 25.3 |
| DML Polar Head Group Region | | | | | | | | | | | | |
| DML Polar Group | 100 | 164 | 349.5 | 1.0 | 164 | 349.5 | 100 | 164 | 349.5 | 0.093 | 153.1 | 326.7 |
| CM Steroid Side Chain | | | | | | | | | | | | |
| CM Steroid Nucleus | | | | | | | | | | | | |
| CM Ester Linkage | | | | | | | 100 | 22 | 51.2 | 0.067 | 1.5 | 3.4 |
| CM Hydrocarbon Chains | | | | | | | | | | | | |
| | DML:CM Model II | | | | | | DML:CM Model III | | | | | |
| DML Hydrocarbon Region | | | | | | | | | | | | |
| DML Hydrocarbon Chain | 77 | 161.7 | 581.8 | 0.933 | 150.9 | 543.0 | 66 | 138.6 | 498.6 | 1.0 | 138.6 | 498.6 |
| CM Steroid Side Chain | | | | | | | | | | | | |
| CM Steroid Nucleus | 86 | 122 | 310 | 0.067 | 8.1 | 20.7 | | | | | | |
| CM Ester Linkage | | | | | | | | | | | | |
| CM Hydrocarbon Chains | 77 | 80.9 | 290.9 | 0.067 | 5.4 | 20.0 | | | | | | |
| DML Polar Head Group Region | | | | | | | | | | | | |
| DML Polar Group | 100 | 164 | 349.5 | 0.933 | 153.1 | 326.7 | 100 | 164 | 349.5 | 1.0 | 164 | 349.5 |
| CM Steroid Side Chain | 100 | 65 | 284 | 0.067 | 4.3 | 18.9 | | | | | | |
| CM Steroid Nucleus | 14 | 20 | 51 | 0.067 | 1.3 | 3.4 | | | | | | |
| CM Ester Linkage | | | | | | | | | | | | |
| CM Hydrocarbon Chains | | | | | | | | | | | | |
| Extra Level DML Hydrocarbon Region | | | | | | | | | | | | |
| DML Hydrocarbon Chains | 23 | 48.3 | 173.8 | 0.933 | 45.1 | 162.2 | 34 | 71.4 | 256.9 | 0.933 | 66.6 | 239.8 |
| CM Steroid Side Chain | | | | | | | 100 | 65 | 284 | 0.067 | 4.3 | 18.9 |
| CM Steroid Nucleus | | | | | | | 100 | 142 | 361.6 | 0.067 | 9.5 | 24.1 |
| CM Ester Linkage | 100 | 22 | 51.2 | 0.067 | 1.5 | 3.4 | 100 | 22 | 51.2 | 0.067 | 1.5 | 3.4 |
| CM Hydrocarbon Chains | 23 | 24.2 | 86.9 | 0.067 | 1.6 | 5.8 | 100 | 105 | 377.8 | 0.067 | 7.0 | 25.2 |

TABLE A-3. Model electron density distributions of CM in DML bilayers[a]

| | DML | Model I | Model II | Model III |
|---|---|---|---|---|
| $x_1$(Å) | 0 | 0 | 2.34 | 3.4 |
| $\bar{n}$ | | | 48.2 | 88.9 |
| $\bar{V}$ | | | 171.4 | 311.4 |
| $(x_1)e^-$/Å$^3$ | | | 0.281 | 0.285 |
| $x_2$ | 9.9 | 9.9 | 9.9 | 9.9 |
| $\bar{n}$ | 210 | 216.8 | 164.4 | 138.6 |
| $\bar{V}$ | 755.5 | 773.5 | 583.7 | 498.6 |
| $(x_2)e^-$/Å$^3$ | 0.278 | 0.280 | 0.282 | 0.278 |
| $x_3$ | 17.9 | 17.9 | 17.9 | 17.9 |
| $\bar{n}$ | 164 | 154.6 | 158.7 | 164 |
| $\bar{V}$ | 349.5 | 330.1 | 349.0 | 349.5 |
| $(x_3)e^-$/Å$^3$ | 0.468 | 0.468 | 0.455 | 0.468 |
| $x_4$ | 26.25 | 26.25 | 26.25 | 26.25 |
| $(x_4)e^-$/Å$^3$ | 0.334 | 0.334 | 0.334 | 0.334 |

[a] See Fig. 8, above.

comprises 100% of the CM ester linkage and 23% of the hydrocarbon chain. Variations on this model also tested were *1*) no cholesteryl myristate components reside in the polar region, and *2*) no extra level of electron density was considered to be present.

Model III assumes that all the cholesteryl myristate exists as a separate level of electron density near the center of the bilayer.

The percent occupancy (%$T$) of cholesteryl myristate in each level was determined from the molecular lengths given in Table A-1. The mole ratio of DML:CM used in the calculation was 15:1 (~5 wt%), from which a multiplicity factor, $\kappa$, was determined to calculate the partial electron content ($\bar{n}_\kappa$) and partial volume ($\bar{v}_\kappa$) for each component occupying a given level. The calculated parameters for the three models are summarized in **Table A-2** and the values of $x$ and $\rho(x)$ for each model are summarized in **Table A-3.**

The continuous transforms were computed after direct integration of the generalized transform

$$F(s) = \frac{2}{d}\int_0^{d/2} \cos(2\pi s \cdot x)dx$$

integrating from 0, $x_1$, $x_2$, . . . , d/2 and are shown in **Fig. A-2.**

## REFERENCES


A1. Reiss-Husson, F., and V. Luzzati. 1964. The structure of micellar solutions of some amphiphilic compounds in pure water as determined by absolute small-angle x-ray scattering techniques. *J. Phys. Chem.* **68:** 3504–3511.

A2. Craven, B. M., and G. T. DeTitta. 1976. Cholesteryl myristate: Structures of the crystalline solid and mesophases. *J. Chem. Soc. (Perkin Ser. II)*: 814–822.

A3. Rand, R. P., and V. Luzzati. 1968. X-ray diffraction study in water of lipids extracted from human erythrocytes. *Biophys. J.* **8:** 125–137.


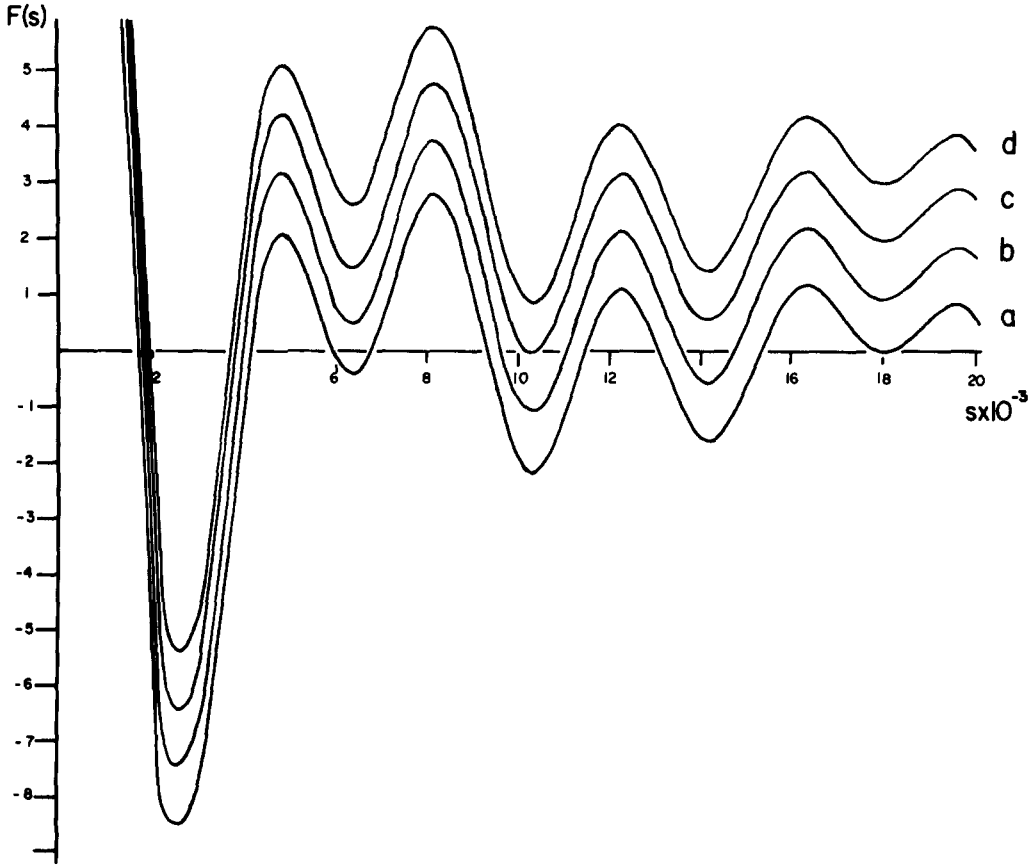


**Fig. A-2.** Calculated Fourier transform $F(s)$ for the models of the organization of cholesteryl myristate in a dimyristoyl lecithin bilayer. *a*) Dimyristoyl lecithin without cholesterol esters; *b*) Model I; *c*) Model II; *d*) Model III. The models and calculations are as described in the text. The transforms have been displaced vertically by one amplitude unit for clarity.